



EFFECT OF PROCESSING TECHNIQUE ON WELDABILITY OF IN738 ALLOY

M.C. Chaturvedi*, R.K. Sidhu and O.A. Ojo

Department of Mechanical and Manufacturing Engineering, University of Manitoba, Winnipeg, Manitoba, Canada R3T 5V6

Abstract

The weldability of IN738 alloy processed by two different casting techniques, viz., conventional casting and directional solidification, was investigated by using autogenous bead-on-plate laser beam welding. Microstructural analysis of the welded samples showed that in both the materials, cracking occurred mainly in the heat affected zone (HAZ). However, the amount of HAZ cracking was observed to be significantly greater in the conventionally cast polycrystalline alloy than that in the directionally solidified (DS) alloy. Besides, cracking in directionally solidified material was observed to be minimum in samples welded in a direction perpendicular to the solidification direction (i.e. the transverse direction), compared to when welding was done parallel to the solidification direction (i.e., the longitudinal direction). The results of this research indicated that an increase in grain size, that is, a reduction in the number of grain boundaries, particularly the transverse grain boundaries, in the material produced by directional solidification vis-à-vis the conventionally cast material can significantly alleviate the problem of HAZ cracking in IN738 superalloy.

1. Introduction

Cast nickel-base superalloy Inconel 738 (IN738) is a high-temperature alloy, precipitation strengthened by coherent precipitates of ordered intermetallic compound $\text{Ni}_3(\text{Al,Ti})$, commonly known as the γ' phase. It is widely used to manufacture hot section components, such as blades of land-based power generation and aero-engine gas turbines. It exhibits an excellent combination of high creep rupture strength and hot corrosion resistance, the two most important requirements for the high-temperature applications. The alloy, which can be used up to a temperature of about 980°C , is generally produced in a conventionally cast i.e., polycrystalline form. In the gas turbine industry, there is always a growing need to develop more advanced versions of superalloys that could withstand increasingly higher operating temperatures and stresses for a better efficiency. Directional solidification process, which produces a columnar grain structure with a preferred $\{001\}$ orientation in nickel-alloys, due to alignment of the grains with the heat flow direction, has been observed to result in alloys with greatly improved properties [1-3]. Directionally solidified (DS) superalloys possess better elevated temperature capability than the conventionally cast polycrystalline alloys due to a reduction or elimination of highly stressed transverse grain boundaries. As a result, DS IN738 alloy not only exhibits better creep rupture properties, but its high temperature ductility and thermal

fatigue resistance are also better than the conventionally cast polycrystalline IN738. Since, welding is commonly used to manufacture complex shaped components with superalloys, the capability of these components to be fabricated as well as repaired by various fusion welding methods would be a very vital factor in the successful commercial application of DS IN738.

In a survey of gas turbine repair organizations located world wide, laser beam welding has been suggested as the process with a significant potential for advanced blade repair technology [4]. It is a relatively new fusion welding technique that offers several advantages over conventional welding methods, such as reduced repair time, lower overall costs, increased flexibility, ability to weld complex structures, and a lower and concentrated heat input which reduces the heat affected zone (HAZ) size [5-6]. However, it is known that high strength γ' precipitation-hardened nickel based superalloys, especially those containing a substantial amount of Al and Ti (>6 at%) are one of the most difficult materials to weld. Application of fusion welding processes to manufacture or repair the components made from these alloys is severely limited by their susceptibility to heat-affected zone (HAZ) cracking during welding and during the subsequent post weld heat treatment (PWHT). High γ' volume fraction in the alloys leads to severe thermal-mechanical strains and stresses during welding or weld cooling due to rapid re-precipitation of γ' particles, causing HAZ cracking.

Corresponding Author: E-Mail: mchat@cc.umanitoba.ca

Courtesy: Proceedings of 2nd international conference on Recent Advances in Material Processing Technology-National Engineering College & Society for Manufacturing engineers, K. R. Nagar, Kovilpatti – 628 503, Tamilnadu, India

Previous research on conventionally cast alloys by other researchers [7-8] and on gas-tungsten-arc welded polycrystalline IN738 by the present authors [9-11] has indicated that in addition to the undesirable effects of high γ' content on weld-cracking, grain boundary liquation microfissuring in weld HAZ is a serious problem during fusion welding of alloys like IN738. As no prior information was available in the literature on the weldability of DS IN738 alloy, the present work was undertaken to examine the weld cracking behaviour of DS IN738 alloy in comparison with the conventionally cast polycrystalline IN738 alloy of an identical composition, during laser beam welding process. The results of this investigation are presented and discussed in this paper.

2. Experimental Details

The nominal composition of IN738 alloy used in this investigation was (wt%) 2.77Al, 3.18 Ti, 14.80 Cr, 8.48 Co, 1.95 W, 1.81 Mo, 4.70 Ta+Nb, 0.1 Si, 0.04 Zr, 0.008 B, 0.004 S, 0.013 P, 0.09 Fe, 0.13 C and balance nickel. It was received in a conventionally cast i.e., polycrystalline form as a cylindrical billet of 85 mm diameter. Weld coupons of size 50x25x3 mm were machined from the as-received billet by a numerically controlled wire electro-discharge machine (EDM). To obtain a directionally solidified (DS) material, the alloy was subsequently re-melted in a Bridgman furnace and directionally solidified in the form of 120 mm long rods of diameter 25 mm, at a withdrawal rate of 2 mm/min. Longitudinal and transverse coupons of 3 mm thickness were cut with EDM by sectioning the as-cast DS rod in a direction parallel and perpendicular to the solidification direction, respectively, for welding. The solidification microstructure in the polycrystalline and DS samples was examined by macro-etching with Marble's reagent (10 gm CuSO_4 + 50 ml H_2O + 50 ml HCl). All the coupons were given a pre-weld heat treatment at 1120°C for 2 hours, which is the standard solution heat treatment used for conventionally cast IN738. The specimens were laser beam welded autogenously, using a laser power of 1.5kW and a welding speed of 2500 mm/min. Subsequent to welding, the coupons were sectioned transversely to the laser beam traversing direction, and prepared for microstructural analysis by using standard metallographic techniques. Specimens were electrochemically etched in a solution of 12 ml H_3PO_4 + 40 ml HNO_3 + 48 ml H_2SO_4 at 6 V for 5 s. The microstructures of the as-cast, solution heat-treated and welded specimens were examined by optical microscope, a JEOL-5900 scanning electron microscope

(SEM) equipped with an Oxford ultra thin window detector energy dispersive spectrometer (EDS), a field emission gun SEM of JEOL Auger microprobe JAMP-9500 and a JEOL-2100F transmission electron microscope (TEM/STEM) equipped with an Oxford ultra thin window detector EDS. Cracking susceptibility of the welds made with polycrystalline alloy, and along the longitudinal and transverse directions of the DS alloy was determined by measuring the length of all the cracks observed in 10 sections of each weld using SEM image analysis software. The nature of grain boundaries in the base metal was determined by electron back scatter diffraction (EBSD) based orientation imaging microscopy (OIM) technique using JEOL-5900 SEM equipped with TSL (TSL, Salt Lake City, UT) OIM system.

3. Results

3.1 Pre-weld microstructure of the alloys

Figure 1a shows an optical macrograph of the as-received conventionally cast polycrystalline IN738 alloy. The grain size of the polycrystalline alloy was found to be between 500-800 μm , with average secondary dendrite arm spacing of $59 \pm 8 \mu\text{m}$. The subsequently re-melted and directionally solidified alloy (DS IN738) was observed to have a well-aligned columnar grain macrostructure along the longitudinal direction, with grains ranging from 70–120 mm in length and 5–10 mm in width. The grains consisted of numerous dendrites parallel (L.S.) and perpendicular (T.S.) to the solidification direction, as observed in the optical macrographs of the as-cast DS IN738 alloy shown in Figure 1b and c, respectively. Average primary and secondary dendrite arm spacings, λ_p and λ_s , in DS IN738 were measured to be approximately 500 ± 29 and $60 \pm 12 \mu\text{m}$, respectively.

The as-cast microstructure of both conventionally cast and directionally solidified alloy was observed to be cored dendritic, with interdendritic regions enriched in Ti, Ta, Nb, Zr and Mo due to micro-segregation during solidification. Extensive precipitation (volume fraction $\approx 42\%$) of the principal hardening phase, the gamma prime (γ') particles, occurred within the dendritic and interdendritic regions (Figures 2a and b). Besides γ' precipitates, the interdendritic regions were observed to contain smaller volume fractions ($\sim 1\text{-}2\%$) of various secondary solidification constituents such as Ti-, Ta- and Nb-rich large, blocky MC-type carbides, Ti- and Zr-rich Sulpho-carbides, $\gamma - \gamma'$ eutectic and some terminal solidification constituents (Figure 2a). The terminal solidification constituents, which mostly formed in the

vicinity of $\gamma - \gamma'$ eutectic islands were found to consist of Cr-, Mo-rich borides and Ni-Zr and Ni-Ti rich intermetallic compounds. These microconstituents, which were observed in both polycrystalline and DS IN738, were identified by micro-chemical analysis with SEM-EDS and TEM-EDS analysis, and their crystal structure determined by TEM-SADP analysis, were reported by the authors in earlier papers [9-12].

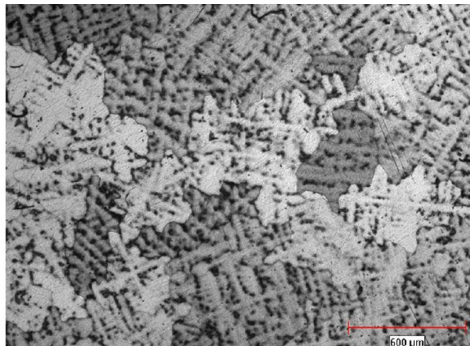


Fig 1a Macrostructure of as-received conventionally cast IN738 alloy

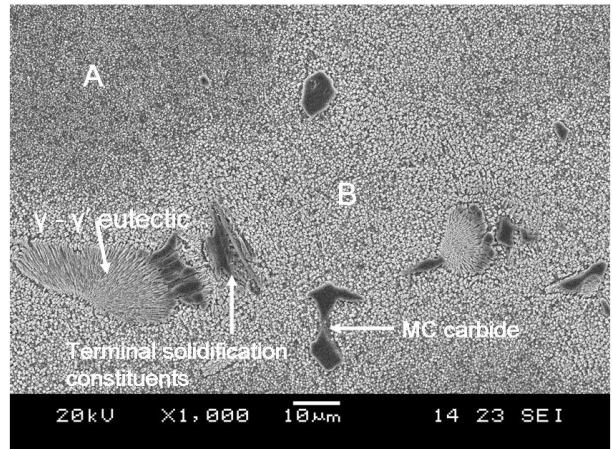


Fig 2a SEM micrograph of as-cast polycrystalline alloy showing secondary solidification constituents (A-dendrite core; B-Interdendritic region)

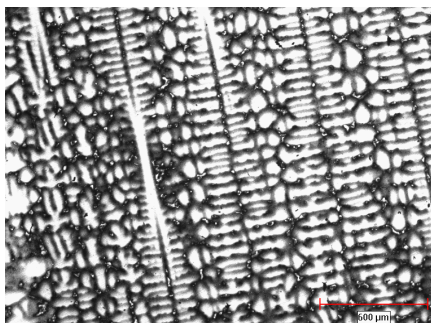


Fig 1b Macrostructure of directionally solidified alloy,

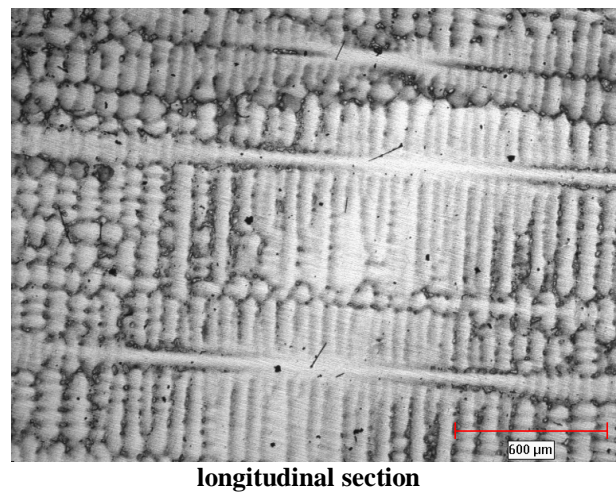


Fig 2b SEM micrograph of as-cast DS alloy showing γ' precipitates (A-dendrite core; B-Interdendritic region)

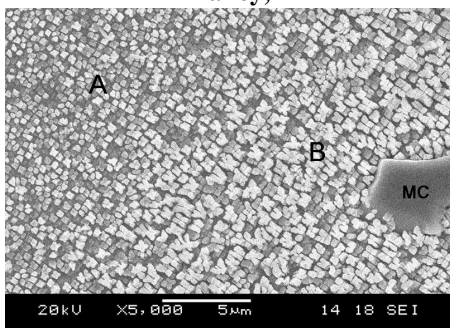


Fig 1c Macrostructure of directionally solidified alloy, transverse section

As seen in SEM micrograph of as-cast DS IN738 at higher magnification (Figure 2b), γ' particles in the dendrite cores (A) varied from 'ogdoadically diced cubes' to nearly rounded cuboidal particles of size 0.3-0.4 μm , whereas the interdendritic regions (B) contained coarser γ' particles in the form of 'ogdoadically diced cube clusters' of size 0.7-0.9 μm . Similar γ' particles were observed in the

polycrystalline alloy except that the interdendritic γ' particles were relatively smaller in size (0.5-0.7 μm). In addition to the core and interdendritic γ' precipitates, fairly large γ' particles of size 1.5-2.0 μm were also observed along the grain boundaries of both materials.

The standard solution heat treatment of polycrystalline and DS IN738 at 1120°C for 2 hours resulted in only a partial dissolution of γ' , as shown in a representative SEM micrograph of DS IN738 in Figure 3. There was almost a complete dissolution of primary γ' in the dendritic regions (A) while only a negligible dissolution of γ' particles in the interdendritic regions (B) was observed. This difference in the dissolution behavior of the core and interdendritic γ' particles has been attributed to solute atom partitioning during solidification. This results in dendrite core γ' being enriched in negatively segregating Al atoms ($k > 1$) and having a solvus of 1120-1130°C, as compared to interdendritic γ' particles that are richer in positively segregating Ti atoms ($k > 1$) and have a higher solvus temperature of 1160-1170°C [13]. During cooling from the solution treatment temperature fine secondary γ' particles precipitated, due to their rapid precipitation rate, predominantly in the dendritic core regions and to a lesser extent in the interdendritic zones. This resulted in the precipitation of small spheroidal γ' particles of 0.1- μm average size in dendrite cores and a bimodal distribution of γ' precipitates in the interdendritic region, consisting of larger cuboidal primary γ' particles of $> 0.5 \mu\text{m}$ and fine spherical γ' particles of approximately 0.1 μm , as seen in Figure 3.

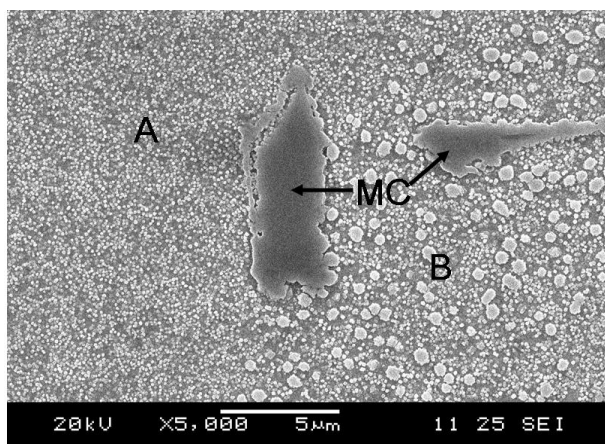


Fig 3 γ' precipitates in SHT DS IN738 (A-dendrite core; B-Interdendritic region)

3.2 Metallography of welded specimens and evaluation of weldability

Figures 4a and b show typical optical micrographs of the laser welded sections of polycrystalline and DS IN738, respectively. As

observed in these figures, no evidence of fusion zone solidification cracking was observed in any of the welded samples. Microfissures or cracks were observed to occur in the HAZ adjoining the weld metal and the cracks were mostly located in the neck region of the welds (Figure 4a). The HAZ microcracks originated close to the fusion line and extended into the base metal to a distance of 150-200 μm . Only a few HAZ cracks were seen to extend partly into the fusion zone (e. g., the crack on left hand side in Figure 4 and the crack in Figure 6). The HAZ microstructure of the welds was extensively examined by SEM-EDS and representative micrographs from the two materials are shown in Figure 5-8. As seen in these micrographs, HAZ microfissures formed along the grain boundaries and had an irregular or zigzag morphology, that is typical of liquation cracks. The crack paths in both polycrystalline and DS IN738 were decorated with re-solidified products of the grain boundary liquid films produced by the constitutional liquation of various microconstituents present in the pre-weld alloys, namely γ - γ' eutectic (Figures 5-7), γ' precipitates (Figure 7) and MC carbides (Figure 5 and 8). Presence of large MC-type carbide particles, which were mostly rich in elements Ti, Nb and W, along a liquated HAZ grain boundary, is shown in the SEM-EDS maps of these elements given in the Figure 8.

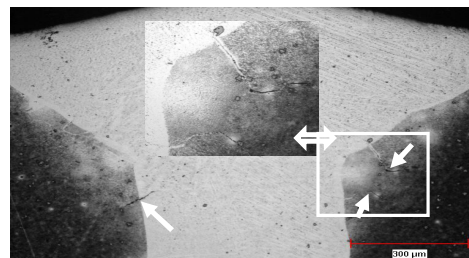


Fig 4a Optical micrograph of polycrystalline IN738 laser weld (3 cracks observed in this section indicated with arrows)

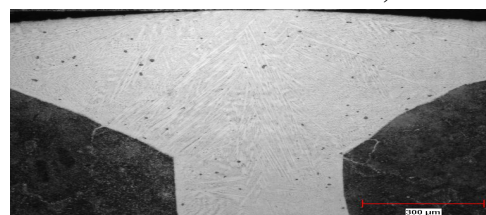


Fig 4b Optical micrograph of DS IN738 laser weld made perpendicular to solidification direction, i.e., T.S. weld (No crack observed on this particular section)

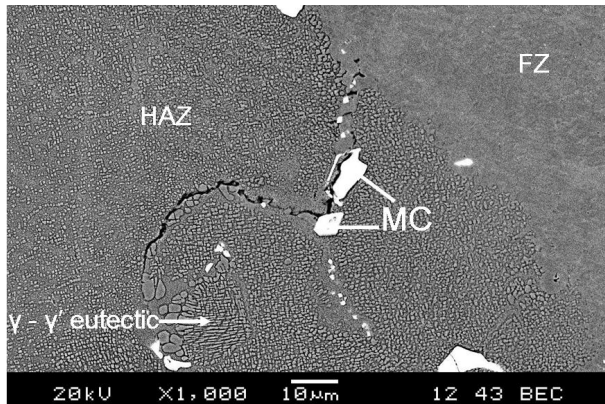


Fig 5 Backscattered electron image showing MC carbides associated with HAZ crack in polycrystalline IN738 weld

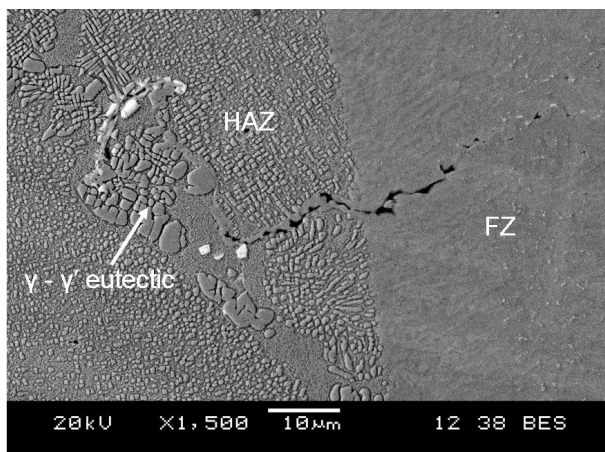


Fig 6 Backscattered electron image showing γ - γ' eutectic and MC carbides associated with HAZ crack in DS IN738 (L.S. weld)

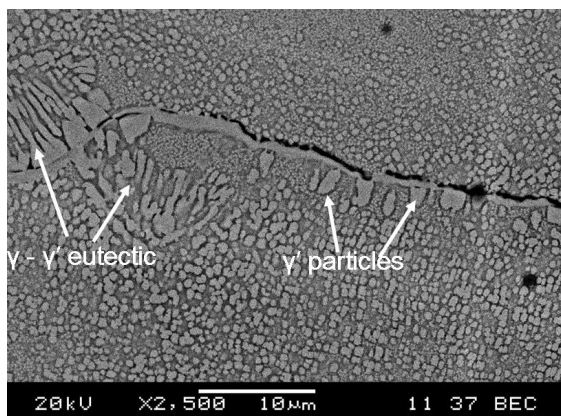


Fig 7 Backscattered electron image showing γ - γ' eutectic and γ' precipitates associated with HAZ crack in DS IN738 (L.S. weld)

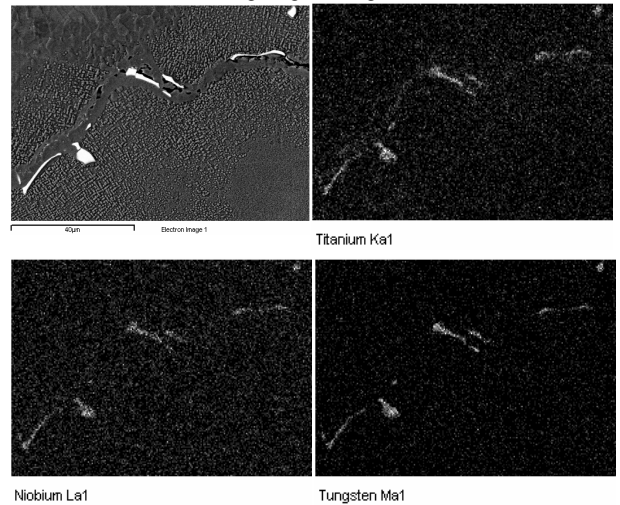


Fig 8 Backscattered electron image showing MC carbides associated with a liquated HAZ grain boundary in polycrystalline IN738 weld, along with EDS maps for Ti, Nb and W

The average total crack length per section (Av. TCL/section) and the average number of cracks per section in different samples are given in Figure 9a and b, respectively. It is seen that a significantly higher degree of HAZ cracking occurred in the polycrystalline IN738 samples than that observed in the DS IN738 samples. Furthermore, in case of DS IN738 alloy, the specimens welded perpendicular to the solidification direction (T.S.) were observed to exhibit a significantly reduced cracking than those welded along the solidification direction (L.S.). The Av. TCL/section (Figure 9a) in DS IN738 welds was found to be less than half ($\sim 324 \mu\text{m}$) of that measured in the polycrystalline IN738 welds ($758 \mu\text{m}$). As seen in Figure 9b, a significantly higher number of cracks i.e., 6.4 cracks/section were observed in the polycrystalline alloy versus 2.4 cracks/section in the L.S. welds of DS IN738. T. S. welds of DS IN738 showed a negligible amount of cracking, as the Av. TCL/section in these samples was only $12 \mu\text{m}$ (Figure 9a), with just 2 cracks in ten sections examined for crack measurements i.e., an average of only 0.2 cracks/section (Figure 9b).

4. Discussion

The microstructural analysis of HAZs showed that in welds of both polycrystalline and DS IN738, the HAZ microfissures were associated with constitutional liquation of various microconstituents present in the

pre-weld alloys. Since both the materials had similar microconstituents, such as γ' precipitates, MC-carbides,

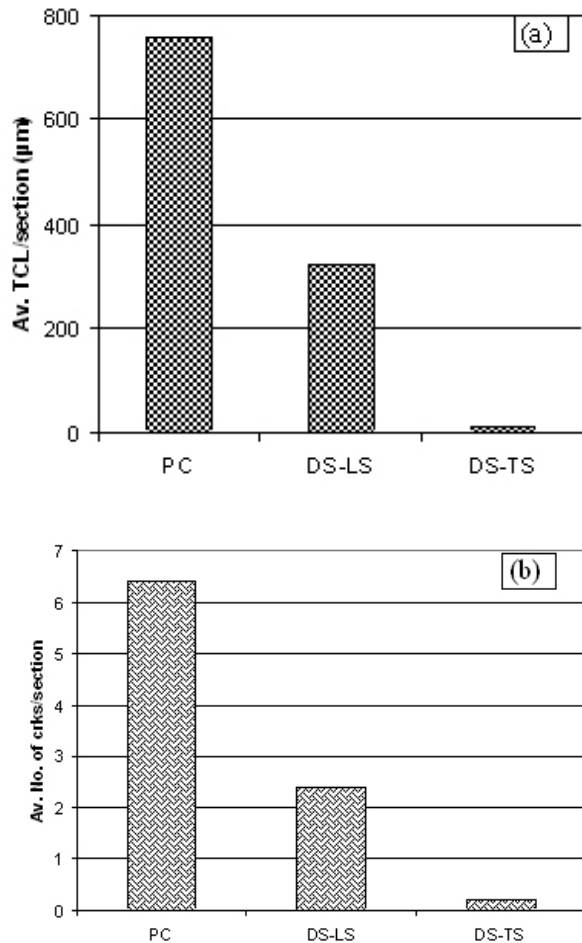


Fig 9 HAZ cracking susceptibility of laser welded samples (a) Average Total Crack Length (Av. TCL) per section and (b) Average Number of Cracks per section

Sulpho-carbides, γ - γ' eutectic and other minor solidification products, these phases were observed to be associated with most of the HAZ microfissures. Liquation of some of these phases present in the two pre-weld alloys is shown in representative micrographs in Figure 5 through 8. These liquation reactions resulted in the formation of solute enriched low melting temperature liquid on the HAZ grain boundaries as observed in the Figure 8. All the HAZ microfissures were found to be intergranular in nature with the characteristic irregular morphology of liquation cracking. Liquation cracking occurs when liquid bearing grain boundaries, where solid-solid bonds have been replaced by weak liquid-solid bonds, are pulled-apart when the tensile component of cooling

stresses exceeds the local strength at such intergranular regions. Hence, the ability of a liquid phase to effectively wet and spread along the grain boundary to form a continuous or semi-continuous film has been observed to be related to the susceptibility of an alloy to liquation cracking during welding.

Analysis of grain boundary microstructure in polycrystalline as well as DS IN738 alloy by orientation imaging microscopy (OIM) technique showed that the majority of the grain boundaries (>97%) in the two materials were high angle grain boundaries. The total fraction of special or coincident site lattice (CSL) boundaries ($\Sigma 3$ - $\Sigma 29$) in polycrystalline and DS IN738 was only 2.9% and 2.7%, respectively. Random or high angle grain boundaries (> $\Sigma 29$) have been observed to have an inherently higher energy than the special or coincident site lattice (CSL) boundaries [14]. Higher grain boundary energy has generally been associated with an improved wettability of grain boundaries. Presence of predominantly high angle random grain boundaries in polycrystalline and DS IN738 could, therefore, be an important factor that would promote extensive grain boundary wetting and penetration by liquid films in the weld HAZ. Moreover, the high angle grain boundaries are also reported to have a lower coalescence temperature [15], which could enhance the stability of the intergranular liquid layer to relatively lower temperatures, thereby aiding the HAZ cracking. In a study on laser welded nickel-base superalloy MC2, the liquid films that formed at high angle grain boundaries were found to be highly prone to the formation of hot cracks [16]. These studies thus suggest that the crack resistance of a material to intergranular HAZ cracking during welding might be improved if the number of crack susceptible high angle grain boundaries in it is reduced. One method to get a lower number of grain boundaries per unit area would be to produce the material by directional solidification casting process.

The alignment of grains during directional solidification produces a significantly large grain size as compared to the polycrystalline alloy, with a resultant reduction in number of grain boundaries in general, and the transverse grain boundaries in particular. Hence, for a weld bead of specific size, a smaller number of grain boundaries will intersect the weld in a DS alloy as compared to a conventionally cast polycrystalline alloy with an essentially equiaxed grain structure with a smaller grain size. A higher probability of grain boundaries intersecting the fusion zone in a polycrystalline alloy would, therefore, enhance its susceptibility to intergranular liquation cracking during welding, as observed in this study. The HAZ cracking susceptibility of welds evaluated by

crack measurements on ten sections of each material showed that the cracking resistance of DS IN738 was significantly better than the polycrystalline IN738 alloy. Both the average total crack length per section (Av. TCL/section) and the average number of cracks per section, shown in Figure 9a and b, respectively, were appreciably reduced in the DS IN738 welded along the solidification direction (L.S.) and almost crack-free welds were obtained in the DS IN738 alloy welded perpendicular to the solidification direction (T.S.). A comparable observation was made by Huang et al [17] in electron beam welds of micro-cast and conventionally cast IN718 alloy, where they found that increasing the grain size in the range of 90-3000 μm resulted in improved weldability. This was related to a lower probability of grain boundaries being intersected by the weld bead, due to reduced number of grain boundaries in the material with a larger grain size, as observed in this study. The observations in the present study as well as those reported by Huang et al [17] are, however, at variance with the previous findings reported in the literature [18-19]. These studies [18, 19] had shown that the weldability of nickel based superalloys could be improved by reducing their grain size as a bigger grain size, in the range of 20-200 μm , was believed to aid HAZ cracking due a longer interface sliding length, larger strain at grain boundary triple points and a larger stress concentration at the grain boundary due to smaller grain boundary area. Contrary to this, the present work has shown that the directional solidification process, which produces cast superalloys with a much larger grain size, and hence, a smaller number of grain boundaries as compared to the conventionally cast polycrystalline superalloys, could in fact help to improve or eliminate the occurrence of weld HAZ microfissuring in highly crack-susceptible IN738 alloy.

5. Summary and Conclusions

1. Laser beam welding of conventionally cast polycrystalline IN738 and directionally solidified IN738 (DS IN738) showed that both versions of IN738 alloy suffered from microfissuring in the heat affected zone, and there was no fusion zone centerline cracking in the welds.
2. The HAZ microfissuring was observed to be closely associated with liquated grain boundaries involving liquation reactions of MC carbides, γ - γ' eutectic and constitutional liquation of γ' precipitate particles, all of

which were present in the pre-weld base metal.

3. The extent of HAZ microfissuring was observed to be significantly less in directionally solidified alloy than that observed in the conventionally cast alloy. This was related to the reduced number of high angle grain boundaries intersecting the weld in DS alloy as compared to those in polycrystalline alloy.
4. The HAZ cracking in DS IN738 was observed to be the least in samples welded in a direction perpendicular to solidification direction (i.e. transverse direction), compared to when welding was done parallel to the solidification direction (i.e. longitudinal direction), which could be attributed to a further reduction in the number of grain boundaries in the transverse direction.
5. Quantitative evaluation of weld microfissuring in IN738 alloy cast by conventional casting and directional solidification showed that the directional solidification process is appreciably beneficial in improving HAZ cracking resistance of IN738 superalloy.

6. Acknowledgements

The authors would like to thank NSERC, the consortium of Manitoba aerospace industries and the University of Manitoba for the financial support, and Standard Aero, Winnipeg for welding the samples.

7. References

1. J.C. Williams and E.A. Starke, "Progress in Structural Materials for Aerospace Systems", *Acta Mater.*, 51, 5775-99, 2003.
2. P. N. Quested and S. Osgerby, "Mechanical properties of conventionally cast, directionally solidified and single-crystal alloys", *Mater. Sci. & Technol.*, 2, 461-75, 1986
3. R. Schafrik and R. Sprague, "The Saga of Gas Turbine Materials I-IV", *Advanced Mater. Processes*, 162, 33-46, 2004
4. D. W. Gandy and J. T. Stover, "Status of weld repair technology for nickel-based superalloy gas turbine blading", EPRI TR-108272 (Electric Power Research Institute, Palo Alto, CA, April 1998).
5. S. Matthiej and M. Hendriks, "Laser welding of industrial gas turbine components", *Sulzer Technical Review*, 86 (1), 15-17, 2004
6. A.D. Williams, and J.L. Humphries "Latest gas turbine repair techniques using laser technology", *Proc. 15th Int. Thermal Spray Conf. 1998, May 25-29, Nice, France*, 2, 1431-35

7. W.A.Owczarski, D.S. Duvall and C.P. Sullivan, "A model for heat-affected zone cracking in Nickel-base superalloys", *Weld. J.*, 45(4), 145-156s, 1966
8. M. Prager and C.S. Shira, "Welding of precipitation-hardening Nickel-base alloys", *Weld. Res. Council. Bulletin, No. 128*, 1-55, 1962
9. O. A. Ojo, N. L. Richards and M. C. Chaturvedi, "Liquation of various phases in HAZ during welding of cast Inconel 738LC", *Mater. Sci. Technol.*, 20(8), 1027-1034, 2004
10. R. K. Sidhu, N. L. Richards and M. C. Chaturvedi, "Effect of aluminium concentration in filler alloys on HAZ cracking in TIG welded cast Inconel 738LC superalloy", *Mater. Sci. Technol.*, 21(10), 1119-1131, 2005
11. R. K. Sidhu, N. L. Richards and M. C. Chaturvedi, "Postweld heat treatment cracking in autogenous GTA welded cast Inconel 738LC superalloy", *Mater. Sci. Technol.*, 23(2), 203-13, 2007
12. R.K. Sidhu, O.A. Ojo and M.C. Chaturvedi, "Microstructural analysis of laser beam welded directionally solidified Inconel 738", *Metall. Mater. Trans. A*, 38A(4), 858-870, 2007
13. R. Rosenthal and D.R.F. West, "Continuous γ' precipitation in directionally solidified IN738 LC alloy", *Mater. Sci. Technol.*, 15(12), 1387-94, 1999
14. H. Grimmer, W. Bollmann and D. H. Warrington, "Coincidence-site lattices and complete pattern-shift lattices in cubic crystals", *Acta. Crystall. A*, A30(3),197-200, 1974
15. M. Rappaz, A. Jacot, and W. J. Boettinger, "Last-stage solidification of alloys: Theoretical model of dendrite-arm and grain-coalescence", *Metall. Mater. Trans. A*, 34A(3), 467-79, 2003
16. N. Wang, S. Mokadem, M. Rappaz, and W. Kurz, "Solidification cracking of superalloy single- and bi-crystals", *Acta Mater.*, 52, 3173-82, 2004
17. X. Huang, N. L. Richards and M. C. Chaturvedi, "Effect of grain size on the weldability of cast alloy 718", *Mater. & Manufg. Processes*, 19(2), 285-311, 2004
18. R G Thompson, "Microfissuring of alloy 718 in the weld heat-affected zone", *J of Metals*, 7, 44-48, 1988
19. R. Thamburaj, W. Wallace and J. A. Goldak, "Post-weld heat-treatment cracking in superalloys", *Int. Met. Rev.*, 28(1), 1-22, 1983.